Symmetry and selection rules in the Raman spectra of carbon nanotubes

T. Yu. Astakhova,[a] G. A. Vinogradov,[a]★ and M. Menon[b,c]

[a]N. M. Emanuel Institute of Biochemical Physics of Russian Academy of Sciences, 4 ul. Kosygina, 119991 Moscow, Russian Federation. Fax: (095) 137 4101. E-mail: gvin@deom.chph.ras.ru
[b]Department of Physics and Astronomy, University of Kentucky, Lexington, Kentucky, 40506-0055, USA
[c]Center for Computational Sciences, University of Kentucky Lexington, Kentucky, 40506-0045, USA. Fax: (859) 323 1029. E-mail: madhu@ccs.uky.edu

The symmetry of achiral single-walled (n,0) and (n,n) carbon nanotubes (CNTs) was examined and the frequencies and types of vibrations allowed in the Raman spectra were calculated. The vibrational spectrum was evaluated as the eigenvalues of the dynamical matrix at the Γ-point of the Brillouin zone. The selection rules for the Raman active vibrations were estimated by the values of the matrix elements responsible for the intensities of corresponding vibrational transitions. The (n,n)-CNTs with even and odd n values are characterized by five and six allowed Raman active vibrations, respectively. The number of Raman active vibrations for (n,0)-CNTs is five if n is even and eight if n is odd. Detailed analysis of the results obtained is presented for the (10,10)-CNT as an example.

Key words: carbon nanotubes, symmetry, Raman scattering.

Carbon nanotubes (CNTs) are highly ordered quasi-1D structures. The existence of different geometric and topological forms of CNTs predetermines most of the interesting properties of these objects.[1—3] Raman spectroscopy is particularly useful for characterization of CNTs with respect to their diameters, chirality, and manifestation of semiconducting or metallic properties. Despite considerable advances in the experimental and theoretical studies of the Raman scattering, there is a number of moot questions. In particular, this concerns the determination of the total number and symmetry of vibrations allowed in the Raman spectra.

It has been assumed for long that, depending on the evenness of the n value,[4] achiral* (n,0)- and (n,n)-CNTs are characterized by a total of 15 or 16 Raman active vibrations, seven of them being intense[5] in the spectral region below 1600 cm^{-1}. Interpretation of the experimental Raman spectra was based on these predictions.[6,7]

Recently,[8] the predicted number of the Raman active vibrations was reduced to eight. This result was obtained using the line group theory[9] developed earlier for isotactic polymers.[10] The necessity of employment of this an approach is due to the fact that none of the point symmetry groups known to date can completely describe the symmetry of CNTs using its own symmetry operations and only the nonsymmorphic* groups permit description of all symmetry operations for CNTs.

In this work we present a detailed analysis of the Raman spectra of achiral single-walled CNTs. A feature of the approach proposed is that it begins with the definition of the eigenvalues (squares of frequencies) and eigenvectors of the dynamical matrix and is free from symmetry restrictions. Allowance of particular normal vibrations in the Raman spectra was determined by evaluating the integrals responsible for the corresponding vibrational transition probabilities. The point is that assignment of a point symmetry group to a particular CNT is rather arbitrary. For instance, the symmetry of the (n,n)-CNTs can be in equivalent manner described by the D_{nh} or D_{nd} groups, though none of them individually can provide a complete description of the symmetry of the CNTs. Naturally, the symmetry assigned to a particular vibrational mode can vary depending on the choice of the symmetry group. Appropriate group theory information[11,12] is used as required.

* Carbon nanotubes in the armchair (n,n) and zig-zag (n,0) conformations are called achiral CNTs.

* Groups for which a complete set of symmetry operations for an object includes both the symmetry operations of the point groups and the spatial translations are called nonsymmorphic groups.

Published in Russian in *Izvestiya Akademii Nauk. Seriya Khimicheskaya,* No. 4, pp. 783—790, April, 2003.

1066-5285/03/5204-823 $25.00

Calculations were carried out using the Brenner empirical potential for hydrocarbons[13] and the Menon semiempirical (tight-binding) scheme.[14,15] Infinite CNTs were simulated by cyclic boundary conditions. Calculations were carried out for achiral $(n,0)$- and (n,n)-CNTs with $n = 9—12$.

Symmetry operations for CNTs

In this section we present necessary information concerning the symmetry of CNTs and consider achiral (n,n)-CNTs with both even and odd n values. Examination of the symmetry of the $(n,0)$-CNTs was performed in a similar way; however, the results obtained are not discussed here because of similarity of the conclusions drawn.

Table 1 gives a complete list of the point symmetry operations for the (n,n)-CNTs with even and odd n values as well as the symmetry operations for the point groups D_{nh} and D_{nd}. The fragments of the (n,n)-CNTs with even and odd n values are shown in Fig. 1, *a*—*c* ($n = 6$) and Fig. 1, *d*—*f* ($n = 5$). Clearly, all (n,n)-CNTs belong to the

Table 1. Symmetry elements of point groups D_{nh} and D_{nd} and symmetry elements of the (n,n)-CNTs with even (I) and odd (II) n values

Symmetry element	D_{nh}		D_{nd}		(n,n)	
	I	II	I	II	I	II
E	+	+	+	+	+	+
C_n^m	+	+	+	+	+	+
S_n^m	+	+	—	—	+	+
S_{2n}^m	—	—	+	+	+	+
σ_v	+	+	—	—	+	+
σ_h	+	+	—	—	+	+
σ_d	+	—	+	+	+	+
C_n'	—	—	+	+	+	+
C_n''	+	+	—	—	+	—
C_n'''	+	—	—	—	+	+
i	+	—	—	+	+	+

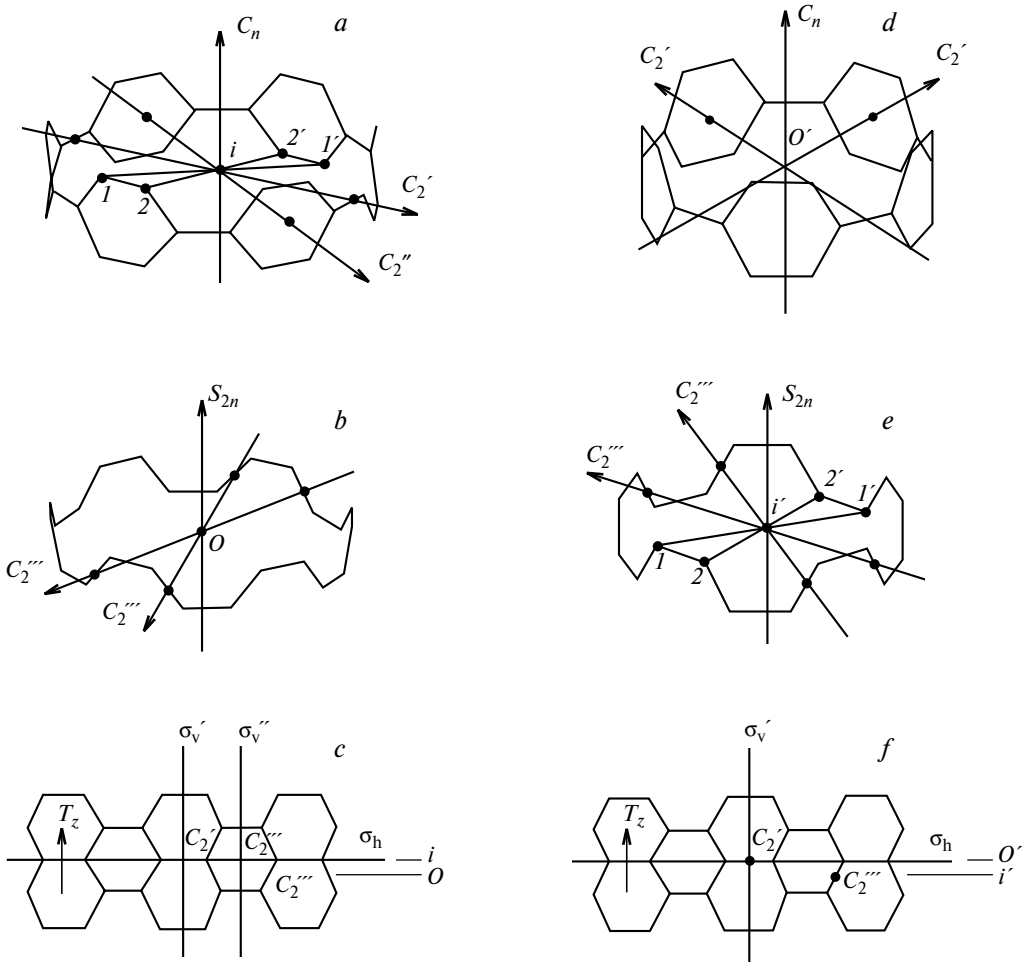

Fig. 1. Symmetry elements of a (6,6)-CNT (*a*—*c*) and a (5,5)-CNT (*d*—*f*). The elementary fragments comprising a chain of hexagons (*a*, *d*) and a cycle in the armchair conformation (*b*, *e*). The developments of the lateral surfaces of these CNTs projected on the hexagonal lattice (*c*, *f*) are also shown.

point symmetry group D_n, since they have an n-fold symmetry axis C_n and n (most often, different) C_2 axes passing perpendicular to the C_n axis: $D_n = C_n \otimes C_2$.

Further assignment to a particular point symmetry group depends on the choice of the elementary fragment.* For instance, let the elementary fragment of a CNT with even n value be chosen in the form of a chain of hexagons (see Fig. 1, *a*). In this case a total of n twofold axes is divided into two classes comprised of $n/2$ axes each. One class of the twofold axes, C_2', passes through the midpoints of the opposite horizontal bonds, while the other class, C_2'', passes through the centers of the opposite hexagons.** There is also a symmetry plane σ_h perpendicular to the C_n axis and passing through the centers of the hexagons. The inversion center, i, coincides with the fixed point. With such a choice of the unit cell the (n,n)-CNT should be assigned to the D_{nh} ($D_{nh} = D_n \otimes \sigma_h$) point symmetry group with the following group generators: C_n, C_2, and σ_h.

If the elementary fragment of a CNT with even n value is chosen in the form of a cycle in the armchair conformation (see Fig. 1, *b*), it has n twofold axes C_2''' belonging to the third class and passing through the midpoints of the opposite slanted bonds. There are also n symmetry planes σ_d passing through the C_n axis and bisecting the angles between the neighboring C_2''' axes. Inversion is absent. With such a choice of the elementary fragment the (n,n)-CNT should be assigned to the point symmetry group D_{nd} ($D_{nd} = D_n \otimes \sigma_d$). In this group, a roto-reflection axis appears, $S_{2n} = C_{2n}\sigma_h'$, where the σ_h' plane is perpendicular to the C_n axis, passes through the midpoints of the slanted bonds, and is shifted downward by $T_z/4$ with respect to the σ_h plane. The translation vector, $\vec{T}_z$, is a spatial symmetry operation (see Fig. 1, *c*) and its length is equal to the distance between the centers of adjacent hexagons along the z axis. The fixed points of the point symmetry groups D_{nh} and D_{nd} are shifted relative to each other by $T_z/4$.

The symmetry of (n,n)-CNTs with odd n values can be analyzed analogously. Depending on the choice of the unit cell, such CNTs also can have a D_{nh} or D_{nd} symmetry (see Table 1, Fig. 1, *d*—*f*).

Examination of the symmetry operations for CNTs and the point symmetry groups D_{nh} and D_{nd} (see Table 1) shows that the CNT symmetry is higher than that of each point group and that none of the groups provides a complete description of the CNT symmetry. The use[8] of the line group theory[9,10] allowed reduction of the number of the Raman allowed vibrations but left some problems for the (n,n)-CNTs unsolved.*

Calculations of vibrational spectra using dynamical matrix

A vibrational spectrum of an arbitrary molecular system can be obtained by solving the matrix equation

$$DX = M\omega^2 BX, \qquad (1)$$

where D is the dynamical matrix, B is the quadratic form of the kinetic energy ($E_{\text{kin}} = 0.5\sum_{i>j} B_{ij}v_i v_j$) ($v_i$ and v_j are the generalized velocities of the atoms i and j, respectively), ω_k and X_k are respectively the frequency and eigenvector of the kth normal mode, and M is the mass of the carbon atom. The matrix elements, D_{ij}, have the form

$$D_{ij} = (\partial^2 E)/(\partial\alpha_i \partial\beta_j), \qquad (2)$$

where E is the potential energy and α_i and β_j are the generalized coordinates of the atoms i and j, respectively. In the Cartesian coordinates the matrix B in Eq. (1) is the unit matrix, I, and the vibrational spectrum is determined by diagonalization of the matrix D. However, it is more convenient to use the cylindrical coordinates $\{z,r,\varphi\}$. Cylindrical symmetry of CNTs allows simplification of the construction of the dynamical matrix: it is sufficient to determine the matrix elements for two adjacent atoms and then breed them for the whole matrix using symmetry operations. The Brenner and Menon potentials employed in this work permit analytical calculations of the second derivatives of the potential energy, which essentially simplifies the procedure for constructing the dynamical matrix and permits refinement of the results obtained.

If a CNT comprises N atoms, the order of the corresponding dynamical matrix is $3N\times3N$ and Eq. (1) has $3N$ solutions. A very large aspect ratio allows the CNTs to be treated as infinite in one dimension. In this case, only the vibrations at the center of the Brillouin zone (Γ-point at $k_z = 0$, the z axis is directed along the CNT axis) are of interest. The modes with $k_z \neq 0$ contribute only to the Raman spectra of finite CNTs.[16,17] As a result, the order of the dynamical matrix is reduced to $3N'\times3N'$, where N' is the number of atoms in the chosen fragment (not necessarily elementary fragment) and $3N'$ is the total number of modes with $k_z = 0$. The eigenvector of the kth normal mode also has $3N'$ components and completely describes its symmetry: for the kth normal mode ($k = 1, 2, \ldots, N'$) the eigenvector of the lth atom ($l = 1, 2, \ldots, N'$) has three values ($\{\breve{z}_k^l, \breve{r}_k^l, \breve{\varphi}_k^l\}$) character-

* An elementary fragment of a CNT is a rectangular fragment constructed on the chiral vectors $\vec{C}_h$ and the translation vector $\vec{T}_z$.[2]

** The choice of the elementary fragment in the form of a chain of hexagons is somewhat incorrect, since the "upper" and "lower" atoms are shared by two adjacent fragments. A way out is to occupy the lattice sites by the halves of atoms.[2]

* The following group structure was proposed to provide a complete description of symmetry: $G[n] = T_z \otimes [D_{nh} \oplus (D_{nd}|_{z=T/4} \ominus C_{nv}) \oplus C_{nv} \otimes S_{2n}]$. The presence of only eight Raman active vibrations was inferred from analysis of this group.

izing the relative displacement of each atom from the equilibrium position. Then, the procedure for the determination of the symmetry of any normal mode becomes readily programmable. Using original code, we found all symmetry operations for each of the $3N'$ normal modes. Special emphasis is placed on the doubly degenerate states, since one should distinguish between the occasional and true double degeneracy of the E modes.

Symmetry of these normal vibrations was determined using conventional rules.[11,12] Nondegenerate modes are labelled A (B) depending on the symmetry (antisymmetry) with respect to the $S_{2n}{}^1$ operation. The states that are symmetric (antisymmetric) with respect to rotation about the C_2 axes are denoted by subscripts 1 (2). The subscripts g (u) were used to label the states that are symmetric (antisymmetric) with respect to inversion i. For the doubly degenerate modes, E_m, the subscript m denotes those types the modes that are transformed using the $S_{2n}{}^m$ symmetry operation.

The achiral CNTs have three classes of twofold axes (C_2', C_2'', and C_2''') passing perpendicular to the principal symmetry axis C_n. There are also modes with "dual" symmetry with respect to the different classes of the C_2 symmetry operations. Namely, such modes are symmetric with respect to one class and antisymmetric with respect to the other class of the C_2 symmetry operations. Figure 2 illustrates this situation taking the Raman inactive mode B_g as an example. The B_g mode is a tangential mode corresponding to equal (in absolute value) displacements of all atoms in each layer* from the equilibrium positions. This mode is antisymmetric with respect to the C_2' and C_2'' symmetry operations and symmetric with respect to the C_2''' operation. Such an ambiguity makes impossible assignment a definite subscript (1 or 2) to the B_g mode. The reason is that the S_{2n} operation requires the smallest structural fragment be comprised of two adjacent atoms. For the same reason we cannot assign particular numerical subscripts to some other modes. It is in this sense that the primitive cell of the (n,n)-CNT comprises two atoms. Below, this will affect the determination of the Raman active vibrations. It should be noted that consideration of the $(n,0)$-CNTs presents no difficulties because of the simpler structure of the elementary fragment (single-atom primitive cell).

Using the above-mentioned symmetry conventions, we calculated complete vibrational spectra of the (n,n)- and $(n,0)$-CNTs with n = 9—12. We started from constructing the dynamical matrices (2) for both potentials employed and then numerically solved Eq. (1). The eigenvalues and eigenvectors of this equation describe a complete vibrational spectrum. The fundamentals in the

* A layer comprises the atoms characterized by equal z-coordinates and lying in the plane perpendicular to the long axis of the CNT.

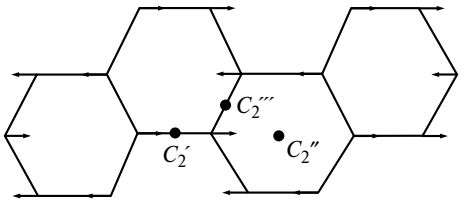

Fig. 2. Tangential vibrational mode B_u corresponding to equal (in absolute value) atomic displacements from the equilibrium positions. Shown are the C_2', C_2'', and C_2''' symmetry axes with respect to which the B_g mode is symmetric or antisymmetric.

calculated spectra of CNTs with even (I) and odd (II) n values are distributed among symmetry species as follows

$$\Gamma_{(n,n)}{}^{I} = 2\,A_{1g} + 2\,A_{2g} + 2\,A_u + 1\,B_{1u} + 1\,B_{2u} + 4\,B_g + 2\,E_{1g} + 4\,E_{1u} + 4\,E_{2g} + 2\,E_{2u} + \ldots + 2\,E_{(n-1)g} + 4\,E_{(n-1)u},$$

$$\Gamma_{(n,n)}{}^{II} = 2\,A_{1g} + 2\,A_{2g} + 2\,A_g + 1\,B_{1u} + 1\,B_{2u} + 4\,B_u + 6\,E_{1u} + 6\,E_{2g} + \ldots + 6\,E_{(n-1)g},$$

$$\Gamma_{(n,0)}{}^{I} = 2\,A_{1g} + 1\,A_{2g} + 3\,A_u + 1\,B_{1u} + 2\,B_{2u} + 3\,B_g + 3\,E_{1g} + 3\,E_{1u} + 3\,E_{2g} + 3\,E_{2u} + \ldots + 3\,E_{(n-1)g} + 3\,E_{(n-1)u}, \quad (3)$$

$$\Gamma_{(n,0)}{}^{II} = 2\,A_{1g} + 1\,A_{2g} + 3\,A_g + 1\,B_{1u} + 2\,B_{2u} + 3\,B_u + 6\,E_{1u} + 6\,E_{2g} + \ldots + 6\,E_{(n-1)g}.$$

The selection rules for the Raman active modes from a complete set of normal modes are considered below.

Determination of Raman active vibrations

Transition probabilities for the Raman scattering are determined using well-known rules.[11] Let ψ_i and ψ_j be the total wave functions of the initial and final states with the energies E_i and E_j, respectively. The probability of the transition $E_i \rightarrow E_j$ is proportional to the square of the transition momentum M_{ij}

$$M_{ij} = \int \psi_j^* \hat{M} \psi_i \mathrm{d}V. \quad (4)$$

In the case of Raman scattering $\hat{M}$ is the dipole moment $\vec{P}$ induced by the external electric field $\vec{E}$ ($\vec{P} = \alpha\vec{E}$, where α is the polarizability tensor). Therefore, determination of the Raman transition probabilities requires calculations of the following integrals

$$\int \psi_j^* \alpha_{\xi\zeta} \psi_i \mathrm{d}V, \quad (5)$$

where $\alpha_{\xi\zeta}$ are the individual components of the polarizability tensor or their combinations and ξ and ζ are the respective Cartesian coordinates. If for at least one component $\alpha_{\xi\zeta}$ the integral (5) differs from zero, the transi-

tion $\psi_i \rightarrow \psi_j$ is allowed. Integration is performed over a complete set of the electron and nuclear coordinates. Calculations of integral (5) in the explicit form is a complicated quantum-chemical problem. At the same time it can be essentially simplified if we are interested in assessment of the allowance of a particular transition in the Raman spectra rather than the values of the transition probabilities.

The total wave functions appeared in integral (5) can be approximately represented as products of the wave functions for the electron motions and the molecular vibrations and rotation, $\Psi = \Psi^{el}\Psi^{vib}\Psi^{rot}$, assuming that these motions are executed independently.[15,18] It is possible to select only the vibrational degrees of freedom (see, *e.g.*, Ref. 18). The corresponding integrals in expression (5) are as follows:

$$\int \psi_j^{vib} \alpha_{\xi\zeta} \psi_i^{vib} dV. \quad (6)$$

The vibrational wave function is a real function and can be represented as an eigenvector of the dynamical matrix. When determining the allowance of vibrational transitions in the Raman spectra at the Γ-point of the Brillouin zone the problem is additionally simplified: it is sufficient to consider the surface integral instead of the volume integral, since there is no dependence on the z coordinate. Then, the integral (6) can be transformed as follows

$$\int \psi_j^{vib} \alpha_{\xi\zeta} \psi_i^{vib} dx dy. \quad (7)$$

In the simplest (and most interesting) case the wave function of the initial state i has an A_{1g} symmetry. Then the considered transition is allowed if at least one component of the polarizability tensor has the same symmetry as does the excited vibrational state j. In other words, allowance of a Raman transition requires that the components of the polarizability tensor behave with respect to symmetry operations in exactly the same way as does the wave function of the excited vibrational state. From this it follows that the totally symmetric mode A_{1g} is always Raman active, since the polarizability tensor always has totally symmetric components.[15] Then, taking into account the fact that the wave function of the totally symmetric mode A_{1g} is a constant, it is sufficient to analyze the following integral

$$\int \psi_j^{vib} \alpha_{\xi\zeta} dx dy. \quad (8)$$

Examination of the components of the polarizability tensor for achiral CNTs (see Appendix) reveals that only the diagonal elements (α_{xx}, α_{yy}, α_{zz}) and the α_{xy} and α_{yx} components ($\alpha_{xy} = \alpha_{yx}$) differ from zero and that the principal axes of the tensor coincide with the natural axes of the CNT, as follows from symmetry considerations. The nonzero components of the polarizability tensor, except for the α_{zz} and $(\alpha_{xx} + \alpha_{yy})$ components having constant values, are shown in Fig. 3.

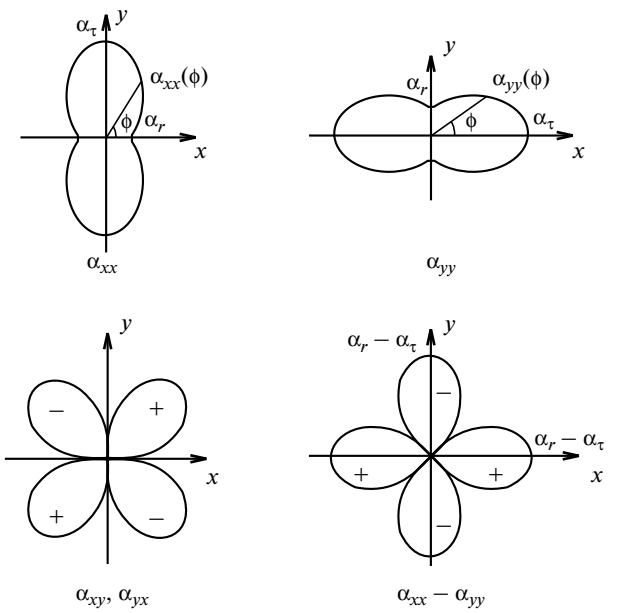

Fig. 3. Schematic representation of the nonzero elements of the polarizability tensor, α_{xx}, α_{yy}, α_{xy}, and $(\alpha_{xx} - \alpha_{yy})$.

Relations between the symmetry of the allowed vibrational mode and the nonzero components of the polarizability tensor have been well documented (see, *e.g.*, Ref. 2). Earlier, the allowance of particular vibrational modes was inferred based on the results of similar examination. This formal approach was found to be inadequate in the case of CNTs, since the symmetry of the polarizability tensor and the vibrational modes can be related only for those molecules which, first, have a definite point symmetry group and, second have a single-atom primitive cell. The achiral CNTs do not fulfil these requirements, since their symmetry cannot be completely described by the point groups and the primitive cell of the (n,n)-CNTs is comprised of two atoms. Therefore, the only way to determine the allowance of a particular vibrational mode in the Raman spectra requires is to evaluate (even qualitatively) the integral (8).

Raman active modes of (10,10)-CNT

Let us apply the proposed strategy for determination of the Raman active modes to the (n,n)-CNTs with even n values taking the (10,10)-CNT as an example. The procedure requires examination of each normal mode and comparison of its symmetry properties with the properties of the components of the polarizability tensor with respect to all symmetry operations of the CNT. In this case, the three nonzero components $(\alpha_{xx} + \alpha_{yy})$, $(\alpha_{xx} - \alpha_{yy})$, and α_{xy} act as "sieve" to pass all the vibrational modes

listed in expression (3). Since in this work we are dealing with the vibrations at the Γ-point of the Brillouin zone (see above), cyclic boundary conditions were used. The (*n*,*n*)-CNTs were simulated by two layers of carbon atoms (a total of 4*n* carbon atoms in the cell). The cell of the (10,10)-CNT contained a total of 40 atoms, while the total number of the vibrational modes, including zero modes, is 120.

The problem of determination of the Raman active modes is essentially simplified, since we can beforehand exclude a large number of the Raman inactive modes. First, these are all modes that are antisymmetric with respect to inversion *i* (labelled by subscript u), since all components of the polarizability tensor are symmetric with respect to this operation.[15]

Second, all the B modes are also excluded since they are antisymmetric with respect to the S_{2n} operation. Since all these modes correspond to equal absolute displacements of all atoms from the equilibrium position, they should be compared with the α_{zz} or $(\alpha_{xx} + \alpha_{yy})$ components of the polarizability tensor, which also have constant values. However, both these components are symmetric with respect to the S_{2n} operation, which means that all the B modes are Raman inactive.

Third, the A_{2g} states are also Raman inactive, since they are antisymmetric with respect to the C_2 symmetry operations, whereas all the nonzero components of the polarizability tensor or their combinations are symmetric with respect to the C_2 symmetry operations. Thus a set of the nondegenerate Raman active modes includes only the A_{1g} modes.

Mention may be made concerning determination of the Raman active modes among all the doubly degenerate normal modes E_{mg} (m = 1, 2, ..., n – 1). As is shown in the Appendix, the $(\alpha_{xx} - \alpha_{yy})$ or α_{xy} components are proportional to $\sin(2\varphi+\Phi)$, where φ is the angle between the x axis and the running direction and Φ is a phase. If atomic displacements from the equilibrium positions are assigned signs, each E_{mg} mode behaves in proportion to $\sin(m\varphi+\psi)$, where ψ is also a phase. Therefore, evaluation of the integral (8) is reduced to calculations of the following integral

$$\int_0^{2\pi} \sin(2\varphi+\Phi)\sin(m\varphi+\psi)\mathrm{d}\varphi, \qquad (9)$$

which differs from zero only at m = 2. Therefore, only four E_{2g} modes are added to the two A_{1g} modes for the (*n*,*n*)-CNTs with even *n* values. Thus, simple considerations show that among all the normal modes listed in expression (3), only the A_{1g} and E_{2g} modes can be Raman active.

Let us consider now the "fine" structure of the vibrational modes with E_{2g} symmetry (Fig. 4) taking the (10,10)-CNT as an example. As can be seen, these modes can be divided into two groups: the modes (*a*), (*b*), and (*d*)

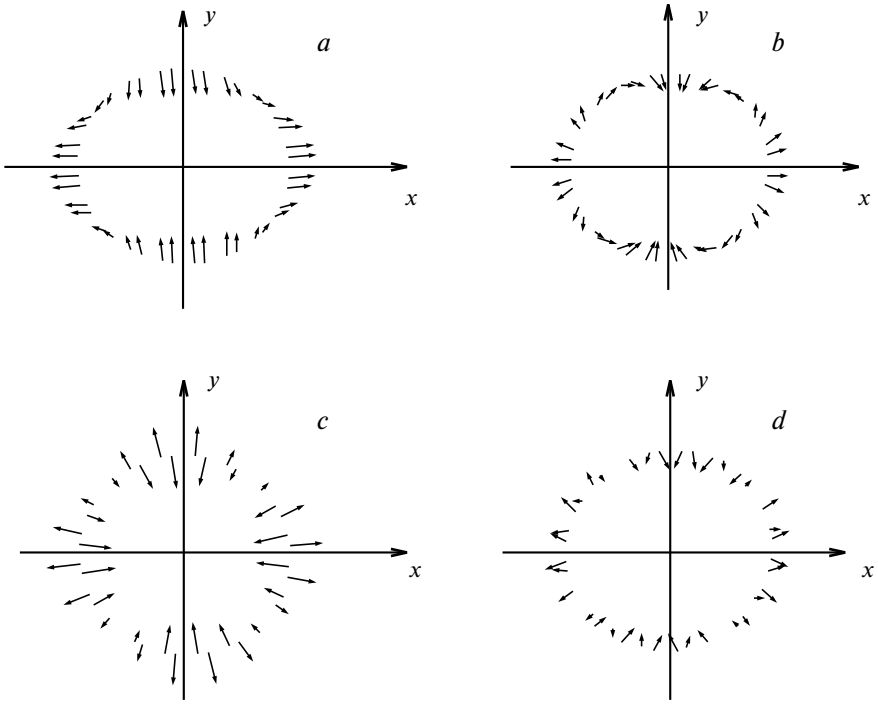

Fig. 4. Schematic representation of all the E_{2g} vibrational modes (*a*—*d*). Arrows illustrate atomic displacements from the equilibrium positions. The modes have a four-lobe shape. The relative direction of the displacement vectors of adjacent atoms is noteworthy. Figure *c* corresponds to the out-of-phase vibrations of adjacent atoms.

belonging to the "in-phase" vibrations, when the vectors of displacement of two adjacent atoms from the equilibrium positions are mainly collinear, and the mode (*c*) characterized by opposite directions of these vectors. This is a consequence of the presence of two atoms in the primitive cell.

Now consider the procedure for evaluating the integrals (8) in more detail. The wave function of the vibrational state in the integral (8) is in fact a discrete set of the vectors of atomic displacements from the equilibrium positions and the integral (8) for the (*n*,*n*)-CNTs can be represented as the sum

$$\sum_{k=1}^{2n} \Psi_j^k(\varphi_k)\alpha_{\xi\varsigma}^l(\varphi_k), \qquad (10)$$

where Ψ_j^k is the discrete wave function of the vibrational state, k is the number of the atom in a particular layer, j labels the type of the normal vibration, and the index l labels the individual components of the polarizability tensor and/or their combinations, which determine the Raman transitions. The argument φ_k explicitly indicates the need of calculations of the products of the atomic displacements from the equilibrium positions and the components of the polarizability tensor at the same angles in the polar coordinates. The sign convention can be made arbitrarily. For instance, the signs of the components of the polarizability tensor can be chosen in accord with formula (14) in the Appendix and the discrete wave function of the vibrational state can be assigned a plus sign if the vector of the atomic displacement from the equilibrium position is directed toward an increase in the radius and the minus sign otherwise.

If for at least one component of the polarizability tensor labelled by index l the sum (10) differs from zero, the corresponding Raman transition is allowed. In the case of achiral CNTs this procedure is simplified, since symmetry of the polarizability tensor and wave function of the vibrational state E_{2g} coincide and their four-petal plots are simply superimposed.

If we superimpose the plot of the $(\alpha_{xx} - \alpha_{yy})$ or α_{xy} components of the polarizability tensor (see Fig. 3) on the plot of the mode (*c*) (see Fig. 4), the sum (10) will be equal to zero because of the alternation of signs of the mode (*c*). From here it follows that the E_{2g} mode is Raman inactive. For the remaining three E_{2g} modes the sum (10) differs from zero.

Thus, analysis of the vibrational modes for the (*n*,*n*)-CNTs with even *n* values shows that only five of them can be Raman active. The calculated frequencies (in cm^{-1}) of the (10,10)-CNT are as follows: 12/17 (E_{2g}), 150/156 ("breathing" mode, A_{1g}), 331/342 (E_{2g}), and two high-frequency tangential modes 1673/1583 (E_{2g}) and 1686/1580 (A_{1g}). Here, the frequencies calculated using the Brenner potential are given in the numerator while those obtained using the Menon potential are given in the denominator.

Similar examination of the (*n*,*n*)-CNT with odd *n* values predicts a total of six Raman active modes ($2\,A_{1g} + 4\,E_{2g}$).

In the case of the zig-zag (*n*,0)-CNT calculations of the Raman active modes are simplified because of the single-atom primitive cell of such CNTs. As a result, the "fine" structure of modes disappears and it is sufficient to determine symmetry of a particular mode to resolve the problem of its Raman activity. Analysis predicts five Raman active modes ($2\,A_{1g} + 3\,E_{2g}$) for the (*n*,0)-CNTs with even *n* values and eight modes ($2\,A_{1g} + 6\,E_{2g}$) for the (*n*,0)-CNTs with odd *n* values.

Note that the results of calculations using the Menon potential are in excellent agreement with the experimental data.

* * *

In this work we presented a strategy of determination of the number of Raman active modes in achiral (*n*,*n*)- and (*n*,0)-CNT. In contrast to earlier studies that predicted eight Raman active modes for each type of CNTs, in this work we have shown that the number of the Raman allowed modes depends on the type of the CNTs and on the evenness of the *n* value. The advantage of the approach employed is exclusion of preliminary complete group theoretical analysis of the symmetry of CNTs and the possibility of determination of the Raman allowed vibrational modes by comparing the signs of the atomic displacements from the equilibrium positions and the components of the polarizability tensor.

The authors express their gratitude to L. A. Gribov (V. I. Vernadskij Institute of Geochemistry and Analytical Chemistry, Russian Academy of Sciences), B. N. Mavrin (Institute of Spectroscopy, Russian Academy of Sciences, Troitsk, Moscow Region), and E. Richter (Daimler-Chrysler, Ulm, Germany) for valuable discussions.

This work was carried out with the financial support from the Russian Foundation for Basic Research (Project Nos. 02-02-16205 and No. 00-15-97334), INTAS (Grant 00-237), National Science Foundation (NSF, Grants NER-0165121 and DMR-9809686), and the U.S. Department of Energy (DOE, Grant 00-63857).

Appendix. Structure of components of polarizability tensor of CNTs

1. Let us consider the non-resonance Raman transitions. For simplicity let the CNT be a thin-walled uniform cylinder of a rather large diameter.

2. Let the external electric field be applied along the *x* axis perpendicular to the vertical axis *z*. Clearly, the electric field can

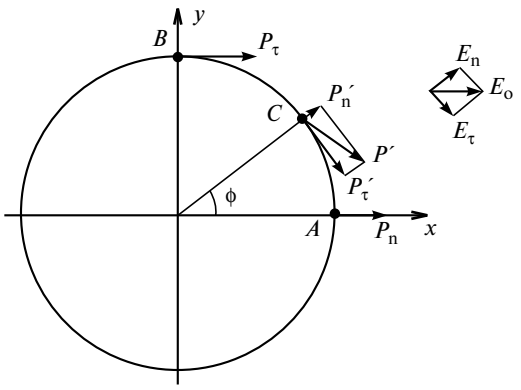

Fig. 5. Components of the electric field and polarizability vector for a cross section of a CNT in the plane perpendicular to the z axis.

not induce polarization along the z axis (at least, for achiral CNTs), since the "top" and the "bottom" of CNTs are equivalent. Therefore, the α_{xz} and α_{yz} components of the polarizability tensor equal zero.

3. Let us examine now how the diagonal (α_{xx}) and off-diagonal (α_{xy}) elements of the polarizability tensor depend on the angles. Consider a cross-section of the CNT in the (xy) plane (Fig. 5). Apparently, at the point A ($\varphi = 0$) the polarization vector has the normal component $\vec{P}_n = a_n\vec{E}$ only, where a_n is the polarizability along the normal direction. For the same reasons, only the tangential component, $\vec{P}_\tau = a_\tau\vec{E}$, exists at the point B ($\varphi = \pi/2$); here, a_τ is the polarizability along the tangential direction. Naturally, the in-plane polarizability of the CNT is larger than the polarizability along the perpendicular direction: $a_\tau > a_n$.

4. Let us consider now a point C. The radius-vector of this point makes an angle φ with the x axis. The electric field at this point has the normal ($E_n = E_0\cos\varphi$) and tangential ($E_\tau = E_0\sin\varphi$) components. The normal and tangential components of the polarization vector at the point C are given by the following expressions

$$P_n' = a_n E_0\cos\varphi, \qquad (11)$$

$$P_\tau' = a_\tau E_0\sin\varphi,$$

while the x- and y-components of the polarization vector $\vec{P}$ at the same point C are

$$P_x' = P_n'\cos\varphi + P_\tau'\sin\varphi, \qquad (12)$$

$$P_y' = P_n'\sin\varphi - P_\tau'\cos\varphi.$$

Substituting the expressions for P_n' and P_τ' given by formulas (11), one gets

$$P_x' = (a_n\cos^2\varphi + a_\tau\sin^2\varphi)E_0, \qquad (13)$$

$$P_y' = (a_n\sin\varphi\cos\varphi - a_\tau\sin\varphi\cos\varphi)E_0.$$

From this it follows that the α_{xx} and α_{xy} components of the polarizability tensor are

$$\alpha_{xx} = a_n\cos(2\varphi) + a_\tau\sin(2\varphi), \qquad (14)$$

$$\alpha_{xy} = -0.5(a_\tau - a_n)\sin(2\varphi).$$

Expressions for the α_{yy} and ($\alpha_{xx} - \alpha_{yy}$) components can be obtained analogously. All the nonzero and non-constant components of the polarizability tensor are shown in Fig. 3.

References

1. M. S. Dresselhaus, G. Dresselhaus, and P. C. Eklund, *Science of Fullerenes and Carbon Nanotubes*, Academic Press, San Diego, 1996.
2. R. Saito, G. Dresselhaus, and M. S. Dresselhaus, *Physical Properties of Carbon Nanotubes*, Imperial College Press, London, 1998.
3. *Carbon Nanotubes*, in *Topics in Appl. Phys.*, Springer, Berlin, 2001, **80**.
4. R. A. Jishi, L. Venkataraman, M. S. Dresselhaus, and G. Dresselhaus, *Chem. Phys. Lett.*, 1993, **209**, 77.
5. R. Saito, T. Takeya, T. Kimura, G. Dresselhaus, and M. S. Dresselhaus, *Phys. Rev., B*, 1998, **57**, 4145.
6. A. M. Rao, E. Richter, S. Bandow, B. Chase, P. C. Eklund, K. A. Williams, S. Fang, K. R. Subbaswamy, M. Menon, A. Thess, R. E. Smalley, G. Dresselhaus, and M. S. Dresselhaus, *Science*, 1997, **275**, 187.
7. C. Journet, W. K. Maser, P. Bernier, A. Loiseau, M. L. de la Chapple, S. Lefrant, P. Deniard, R. Lee, and J. E. Fischer, *Nature (London)*, 1997, **388**, 756.
8. O. E. Alon, *Phys. Rev., B*, 2001, **63**, 201403R.
9. M. Damnjanovic, I. Milosevic, T. Vukovic, and R. Sredanovic, *Phys. Rev., B*, 1999, **60**, 2728.
10. I. Milosevic, R. Zivanovic, and M. Damnjanovic, *Polymer*, 1997, **38**, 4445.
11. R. L. Flurry, *Symmetry Groups. Theory and Chemical Applications*, Prentince-Hall, New Jersey, 1980.
12. M. A. El´yashevich, *Atomnaya i molekulyarnaya spektroskopiya* [*Atomic and Molecular Spectroscopy*], Editorial URSS, Moscow, 2001 (in Russian).
13. D. W. Brenner, *Phys. Rev., B*, 1990, **42**, 9458.
14. M. Menon, K. R. Subbaswamy, and M. Sawtarie, *Phys. Rev., B*, 1993, **48**, 8398.
15. M. Menon, E. Richter, and K. R. Subbaswamy, *J. Chem. Phys.*, 1996, **104**, 5875.
16. R. Saito, T. Takeya, T. Kimura, G. Dresselhaus, and M. S. Dresselhaus, *Phys. Rev., B*, 1999, **59**, 2388.
17. E. Richter and K. R. Subbaswamy, *Phys. Rev. Lett.*, 1997, **79**, 2738.
18. E. B. Wilson, J. C. Jecius, and P. C. Cross, *Molecular Vibrations. The Theory of Infrared and Raman Vibrational Spectra*, McGraw-Hill, New York—London—Toronto, 1957.

Received May 29, 2002;
in revised form October 24, 2002